



The Possible Ameliorative Effect of Nanocurcumin on Di-Ethylhexyl Phthalate-Induced Injury in the Renal Cortex of Adult Albino Rats (A Histological and Biochemical Study)

Nahla E. Ibrahim¹, Asmaa A.A. Kattaia¹, Omnia M. Mohamed^{1*}, Mohamed A. Shaheen¹

¹Department of Medical Histology and Cell Biology, Faculty of Medicine, Zagazig University, Egypt.

*Corresponding author:

OmniMansour

Mohamed

Email:

mone_hinata@yahoo.com

SubmitDate:22-02-2025

Revise Date:21-03-2025

Accept Date:24-03-2025

ABSTRACT

Background: One of the majorities of widely used phthalates is Di-(2-ethylhexyl) phthalate (DEHP), a synthetic industrial chemical that has become a global pollutant. DEHP has harmful effects on various body organs, especially the kidney. Compared to native curcumin, Nanocurcumin, a form of the herb in nanoparticle form, is more soluble, better absorbed, has a higher cellular uptake efficiency, requires lower dosages, and more precisely targets the affected tissue to exhibit its therapeutic effects. Our aim was to assess the ameliorative effect of Nanocurcumin on Di-Ethylhexyl Phthalate-induced injury in rats' renal cortex.

Methods: Twenty-five adult male albino rats were classified to three groups as following : group I control group (15 rats) divided into three subgroups: [subgroup Ia remained untreated until the experiment's end, subgroup Ib given corn oil as 5 mL/kg per day and subgroup Ic given nanocurcumin at dose of 100 mg/kg per day dissolved in distilled water orally for 28 days consecutively], group II (5 rats) (DEHP group) given DEHP at a dose of 500 mg/kg per day orally dissolved in corn oil for 28 days consecutively, group III (5 rats) (Nanocurcumin-treated group) given Nanocurcumin at dose of 100 mg/kg per day dissolved in distilled water orally for 28 days consecutively in combination with DEHP in the same way as group II. Blood samples were obtained for kidney function tests. Biochemical investigation for MDA & SOD were done. Kidney tissue was prepared for H&E, Sirius red stains, immunohistochemical staining for Desmin and β -catenin and electron microscope examination. Statistical and morphometrical studies were conducted.

Results: DEHP group revealed degenerative histological changes included distorted glomeruli and tubules with darkly stained nuclei and vacuolated cytoplasm. Ultra-structural examination of the same group showed thick basement membrane, rarified cytoplasm, disorganized apical microvilli with disorganized basal enfolding and mitochondria. Increased area% of Sirius red, Desmin and β -catenin was detected. Regarding urea, creatinine and MDA levels showed the highest mean values in DEHP group while SOD level was decreased. Following Nanocurcumin treatment, there was an improvement in histological, immunohistochemical and biochemical alterations of the kidney which induced by DEHP.

Conclusions: Nanocurcumin has an ameliorative effect on DEHP induced renal cortical injury via its anti-apoptotic and anti-inflammatory effects. So, Nanocurcumin could be a possible modality in treating chronic kidney disease (CKD).

Keywords: Nanocurcumin, DEHP, EDCs, Renal cortical injury; kidney function test.

INTRODUCTION

Synthetic chemicals called "endocrine disrupting chemicals" (EDCs) have the ability to disrupt the body's natural hormones and cause a variety of diseases in humans, including those related to development, reproduction, the nervous system, the cardiovascular system, the immune system, and metabolism. Environmental pollutants, industrial chemicals, plasticizers, and artificial preservatives are examples of EDCs (1, 2, 3).

About half of the plasticizer produced worldwide is made of Di (2-ethylhexyl) phthalate (DEHP), among the majority of widely utilized phthalates. As a result, DEHP is now one of the most common pollutants in the world. In the manufacturing of plastics, DEHP is a synthetic industrial chemical that makes polyvinyl chloride (PVC) materials more flexible (4, 5).

DEHP is utilized in perfumes, PVC plastics, which are used in medical devices, food packaging, blood storage bags, and household items like toys, floor tiles, furniture upholstery, cables, garden hoses, wall coverings, and gloves. Additionally, DEHP is the most commonly used plasticizer in PVC medical equipment, such as equipment for extracorporeal circulation, hemodialysis tubes, infusion tubes, respiratory tube systems, endotracheal intubations, blood storage bags, and devices for blood exchange and transfusion. Following their widespread use, phthalates can also be found in food, water, and air (6,7, 8).

Nevertheless, DEHP is continually discharged to the environment through manufacturing operations and from finished products due to its noncovalent bond with these materials. DEHP poses an imminent threat to human health because it can enter the body through the mouth, nose, or skin over time. DEHP's known toxicity has led to its prohibition in a number of products, including food contact materials, all over the world (9, 10).

Since the kidney is responsible for concentrating and filtering the majority of environmental pollutants, it is more vulnerable

to them than other organs. Therefore, compared to other organs, the kidney is more exposed to all chemicals and more susceptible to EDCs. EDCs have the potential for accumulation up in the bloodstream and harm the kidneys (11).

Nanotechnology is the study of creating nanoparticles with sizes between 1 and 100 nm by modifying their size, particle structure, and various synthetic methodologies. A major revolution in medical and healthcare treatments and therapies is anticipated as a result of the technological advancement of nanoscale material control. Additionally, there has been an unexpected increase in the use of nanoparticles recently in a variety of fields, including physics, organic and inorganic chemistry, molecular biology, medicine, and material science (12, 13).

A modified form of curcumin known as Nanocurcumin is created by converting curcumin particles into nanoparticles that are more soluble and absorbable by the body. In order to improve drug delivery and expedite treatment without waste or adverse effects, these particles have been demonstrated to be more targeted to the tissue of interest (14).

Nanocurcumin has antioxidant, antimicrobial, anti-inflammatory and anti-neoplastic properties. It has recently been proposed as a prophylactic and therapeutic agent. It is effective against cancers, brain tumors, liver and heart diseases. When compared to free curcumin, Nanocurcumin has a superior ability to remove free radicals and enhanced anti-lipid peroxidation. Concerning its small size and large surface area, Nanocurcumin is capable of preventing and curing a variety of diseases (15, 16).

Accordingly, this study was done to assess the ameliorative effect of Nanocurcumin on Di-Ethylhexyl Phthalate-induced injury in rats' renal cortex.

METHODS

Animals

Twenty five adult male albino rats aged 3 months, weighing between 180 -200 grams. Rats were acquired from the Animal House at

Zagazig University, Faculty of Medicine, Egypt. They were kept in an environment with a regulated temperature of 25–27°C, a 12-hour light/dark cycle, and an approximate humidity level of 40–70%. The animals had free access to clean water and were fed a standard rat chow. A week was spent acclimatization the rats.

Approval for Ethics

All institutional and worldwide guidelines for the care and use of animals were strictly adhered to. The Zagazig University IACUC Committee reviewed and approved the experiment's protocol, which had the approval number ZUIACUC/3/F/107/2023.

Chemicals

Di (2-ethylhexyl) phthalate ($C_{24}H_{38}O_4$) (DEHP, CAS no 117–817; purity ≥ 99) was purchased from Sigma-Aldrich chemicals CO (ST. Louis, MO). DEHP was provided as a viscous liquid.

Nanocurcumin was purchased from NanoTech, Egypt for Photo-Electronics, in the form of nanopowder. Product Code:4020, with particle size 50 ± 5.5 nm.

Characterization of Nanocurcumin

The size and shape of Nanocurcumin were investigated using JEOL JEM 2100 transmission electron microscope (Jeol Ltd, Tokyo, Japan) in Electron Microscope Research Laboratory (EMRL) of Faculty of Agriculture, El Mansoura University, Egypt. The aqueous dispersion of nanoparticles was dropped on a carbon-coated copper grid, which was then dried and inspected using the electron microscope.

Experimental design

Twenty Five rats were divided into three groups

1. Group I (control group) This group consisted of 15 rats and were equally divided into 3 sub-groups (5 rats in each):

- a. **Subgroup Ia (negative control):** did not take any treatment.
- b. **Subgroup Ib (Vehicle control group)** supplied corn oil as 5 mL/kg per day. So, every rat was given 1 milliliter of corn oil (the vehicle for DEHP) orally for 28 days consecutively (17).

c. Subgroup Ic (Nanocurcumin group): given Nanocurcumin at dose of 100 mg/kg per day dissolved in distilled water orally for 28 days consecutively. So, 100 mg Nanocurcumin were dissolved in 100 ml distilled water and each rat received 20 ml distilled water /day containing 20 mg Nanocurcumin (18, 19, 20).

2. Group II (DEHP group) This group included five rats which were given DEHP in a dose of 500 mg/kg per day orally dissolved in corn oil for 28 days consecutively (21). So, 500 mg DEHP were dissolved in 5 ml corn oil and each rat given 1 milliliter of corn oil per day that contains 100 mg of DEHP.

3. Group III (Nanocurcumin-treated group) This group included five rats that were given Nanocurcumin at dose of 100 mg/kg per day dissolved in distilled water orally for 28 days consecutively in combination with DEHP in the same way as group II (18, 19, 21). So, 100 mg Nanocurcumin were dissolved in 100 ml distilled water and each rat received 20ml distilled water /day containing 20 mg Nanocurcumin (20).

Sampling

At the end of the 28th day, body weight of rats of all groups were also estimated then the rats were anaesthetized with 60 ml/kg of phenobarbitone then blood samples were collected. Blood samples were obtained from the retroorbital veins, which were then collected in tubes containing plain (for serum preparation) then they were sacrificed (22). Then, both kidneys were extracted and prepared for histopathological and biochemical procedures.

Biochemical investigations

1. Preparation of tissue for biochemical procedures

Kidney samples were weighed and homogenized with a power homogenizer, (Janke and Kunkel, Germany), into ten parts (w/v) with fifty mM Tris-HCl at pH 7.4. Homogenates were centrifuged at 4,000 rpm for fifteen minutes at 4°C. The supernatant has been preserved at -80 °C for various biochemical assays (23, 24).

2. Estimation of malondialdehyde (MDA) and superoxide dismutase (SOD) activities

The activities of MDA and SOD were calculated by ELISA reader (Absorbance Microplate Reader ELx 800TMBioTek®, Seattle, WA, USA). The results were expressed as MDA (nmol/g protein) and SOD (U/mg protein) (25, 26).

3. Estimation serum creatinine and blood urea nitrogen (BUN)

Following the manufacturer's instructions, the estimation has been completed by the use of commercially available kits (ACCUREX, Biomedical Pvt. Ltd). (27).

Histological study

Kidneys were taken for examination by light and electron microscopes.

1. Light microscopic technique

Kidneys were thoroughly dissected and immediately submerged in buffered formalin for 48 hours then processed to prepare 5 to 7 micrometers in thickness paraffin sections and then stained with Hematoxylin and Eosin for histopathological analysis, Sirius red for demonstration of collagen fibers distribution and immune histochemical stains for Desmin and β -catenin. Digital cameras were utilized to take images and an Olympus microscope was used for examination (28).

2. Immunohistochemical stain

According to the manufacturer's instructions, the avidin–biotin peroxidase system was performed (Thermo Scientific, USA, Cas No. 32020). Primary and secondary antibodies were applied to the 5 μ m-thick sections. The primary antibody for Desmin, a marker for podocyte injury, is Desmin antibody, which is rabbit polyclonal antibody with catalogue number: PA5-16705 with dilution 1:200; Invitrogen, Thermo Fisher Scientific, Waltham, MA USA. β -catenin which is a marker for tubular injury. Using β -catenin antibody for detection of catenin protein. It is a rabbit polyclonal antibody with catalogue number: YPA-1340 with dilution 1:200; Chongqing Biospes Co., Ltd., Chongqing, China. Staining allowed to detect brown positive reactions. Cardiac muscle sections were used as a positive control for

Desmin using (Cat. #ab15200). Colon sections were used as a positive control for β -catenin using (clone E247, Cat. #ab32572). Negative control sections of the kidney were processed in the above-mentioned steps but the primary antibody was not added in this step (Instead, P.B.S was used). Sections were counter stained with Mayer's hematoxylin (29).

3. Transmission electron microscope technique

The specimens were immediately fixed in 2.5%, phosphate buffered glutaraldehyde for 2 hours, then postfixed in 1% osmium tetroxide in the same buffer at pH 7.4 and 4 °C for 2 hours. Specimens were then dehydrated and embedded in epoxy resin. Leica ultra-cut UCT was used to make ultrathin sections (50 nanometers in thickness), which were subsequently stained with lead citrate and uranyl acetate. In the Electron Microscopy Unit of the Faculty of Agriculture, El Mansoura University in Egypt, JEOL JEM 2100 transmission electron microscope (Jeol Ltd, Tokyo, Japan) was used to examine and photograph the ultrathin sections (30).

Morphometric analysis

FIJI image processing software, which is an open-source propagation of Image J2 [General Public License GNU], was used for morphometric analysis. Unaware of the experiment, the examiner conducted the measurements. Five images for five non overlapping unpredictable fields were measured at 400 \times magnification for all rats in all groups. Area percentage % for collagen fibers in Sirius red stained-sections, Area percentage % of both Desmin and β -catenin immunoreaction were measured.

Statistical Analysis

The recorded data was analyzed using IBM SPSS version 23, a statistical program for social sciences. The statistical information was presented as mean \pm standard deviation (SD). A one-way analysis of variance (ANOVA) was utilized to evaluate the variations in the experimental groups' mean values, and the groups were compared using the least significant difference (LSD). P values were

considered highly significant when less than 0.001 and significant when less than 0.05 (31).

RESULTS

The histopathological, immunohistochemical, biochemical and morphological results represented from all subgroup of control group were similar. As a result, we expressed control based on subgroup Ia results.

Characterization of Nanocurcumin

The obtained Nanocurcumin was most spherical with diameters less than 100 nm (average particle size between thirty and sixty nanometers). Using Malvern Zeta sizer ZS (Malvern Instruments, UK, Nawah Scientific Egypt) to measure the surface zeta potentials and sizes of the Nanocurcumin determined by dynamic light scattering (DLS). The results of the zeta potential of nanocurcumin (-12.5 mv) indicated the moderate stability of the prepared nanocurcumin (Figure 1s).

General observational and body weight results (Table 1)

Throughout the duration of the experiment, none of the animals in the study groups died as a result of their treatments. The body weight varied significantly among the three groups in the present study, DEHP group showed highly statistically significant decrease in body weight comparing to other groups. On the contrary, Nanocurcumin-treated group showed highly statistically significant increase in comparison with DEHP group. Without statistically significant difference in body weight among control group and Nanocurcumin-treated group.

Biochemical results (Table 1)

1. Kidney function test

Statistical analysis for the mean values of serum creatinine and serum urea showed that there was highly statistically significant rise in the DEHP group (as the P value < 0.001) comparing to control and Nanocurcumin-treated group. While highly statistically significant decrease were detected in Nanocurcumin-treated group compared to the DEHP group. However, the Nanocurcumin-treated group revealed a non-significant difference when compared to the control group

2. Estimation of malondialdehyde (MDA) (Table 1)

Statistical analysis for the mean values of MDA in the renal tissue revealed that there was statistically significant increase in DEHP group comparing to control and Nanocurcumin-treated groups, with statistically significant difference (p. value 0.003). On the contrary, there was significant decrease in Nanocurcumin-treated group in comparison with the DEHP group, with statistically significant difference (p. value 0.014). However, Nanocurcumin-treated group showed non-significant difference in comparison with control group.

3. Estimation of superoxide dismutase (SOD) (Table 1)

Statistical analysis of the mean values of SOD in the renal tissue showed that there was highly statistically significant difference between the studied groups. Measurements of SOD levels revealed a highly significant decrease in the DEHP-treated group ($P < 0.001$) compared to the control group and Nanocurcumin-treated group. On the contrary, the Nanocurcumin-treated group showed significant increase ($P < 0.001$) in comparison to DEHP group. No statistically significant difference was seen among the control group and Nanocurcumin-treated group.

Histological results

1. Hematoxylin and Eosin stain results: (Figure 1)

Examination of Hematoxylin and Eosin-stained renal cortex sections in adult male rats from the control group revealed normal glomeruli surrounded by Bowman's space. Bowman's capsule was lined with simple squamous cells. The proximal and distal convoluted tubular cells were seen with vesicular nuclei and acidophilic cytoplasm (Figure 1a). Regarding to DEHP group sections showed renal tubular cells with cytoplasmic vacuolation and dark stained nuclei. Other tubules revealed desquamated epithelial cells in their lumen. The glomeruli appeared with congestion (Figure 1b). The renal cortex showed most of tubules contained acidophilic material in their lumen

with dark stained nuclei (Figure 1c). Thickened wall blood vessels and congested blood vessels could be seen. Glomeruli with congestion surrounded by wide Bowman's space were also observed (Figure 1d). Infiltrating inflammatory cells and segmented glomeruli were also observed (Figure 1e). Nanocurcumin-treated group examination showed nearly normal glomeruli, the capsule of Bowman was lined with simple squamous cells and the space of Bowman was approximately normal. Also, proximal and distal convoluted tubular cells were almost normal with vesicular nuclei and acidophilic cytoplasm (Figure 1f).

2. Sirius red stain results: (Figure 2)

Examination of Sirius red stained sections from renal cortex for control group revealed sparse collagen fibers surrounding the kidney's tubules and corpuscles and within capillaries of glomeruli (Figure 2a). While DEHP group revealed increased collagen fibers surrounding the kidney's tubules and corpuscles, within capillaries of glomeruli and along the blood vessels' wall (Figure 2b). In Nanocurcumin-treated group revealed some collagen fibers were deposited surrounding the kidney's tubules and corpuscles and within capillaries of glomeruli (Figure 2c). Bar charts of the mean level of tissue Sirius red (Area%) of different studied groups (Figure 2d).

3. Immunohistochemical staining for Desmin and β -catenin results: (Figure 3)

Immunohistochemical stained sections for Desmin from the renal cortex for control group revealed very few immunoreactions in podocyte's cytoplasm (Figure 3a). DEHP group showed abundant positive brown immunoreactions in podocyte's cytoplasm (Figure 3b). While Nanocurcumin-treated group showed brown positive immunoreactions in some podocytes' cytoplasm (Figure 3c). Bar chart of the mean level of tissue Desmin (Area%) of different studied groups (Figure 3d). Then immunolocalization of β -catenin of control group sections showed scanty brown immunoreactions in renal tubular cells' cytoplasm (Figure 3e). While DEHP group revealed many positive brown

immunoreactions in renal tubular cells' cytoplasm (Figure 3f). Nanocurcumin-treated group showed moderately positive brown immunoreactions in renal tubular cells' cytoplasm (Figure 3g). Bar chart of the mean level of tissue β -catenin (Area%) of different studied groups (Figure 3h).

4. Ultrastructural results: (Figure 4, 5, 6)

Electron microscopic examination of the proximal convoluted tubular cells for control group revealed the proximal convoluted tubular cells rested on a thin, regular basement membrane and had regularly seen euchromatic nucleus and apical microvilli. The cells' basal parts revealed tightly packed parallel organized mitochondria along with basal infoldings (Figure 4a). **DEHP group** showed a part of proximal convoluted tubular cells with small irregular heterochromatic nuclei, disorganized apical microvilli and areas of rarified cytoplasm with some vacuoles. The cell's basal part revealed ill-organized mitochondria and basal infoldings. Thick basement membrane and blood capillary could be seen (Figure 4b).

Nanocurcumin-treated group showed a part of the lining epithelium for proximal convoluted tubular cell rested on thin, regular basement membrane and had regularly seen euchromatic nucleus and apical microvilli. The cell's basal part revealed numerous mitochondria along with nearly regular basal infoldings. Cytoplasmic vacuoles were still observed (Figure 4c).

Electron microscopic examination of the distal convoluted tubular cells for control group revealed the distal convoluted tubular cells rested on a thin, regular basement membrane and had regularly seen euchromatic nucleus. The cells' basal parts revealed tightly packed parallel organized mitochondria along with basal infoldings (Figure 5a). **DEHP group** showed a part of a distal convoluted tubular cell had euchromatic nucleus and regions of rarified cytoplasm with some vacuoles. The cell's basal part revealed ill-organized mitochondria and basal infoldings. Thick basement membrane could be seen (Figure 5b). **Nanocurcumin-treated group** showed a part of a distal

convoluted tubular cell rested on thin, regular basement membrane and had regularly seen euchromatic nucleus. The cell's basal part revealed nearly organized mitochondria along with nearly regular basal infoldings. Cytoplasmic vacuoles were still observed (Figure 5c).

Electron microscopic examination of the blood renal barrier for control group revealed the primary podocyte processes that emerged from the cell body. The filtration barrier was made up of glomerular capillaries' fenestrated endothelium, a thin, uniform glomeruli's basement membrane, and numerous thin pedicels. In the glomerular capillary's lumen, red blood corpuscles were noticed (Figure 6a). **DEHP group** showed disruption of the filtration barrier resulting from thickened, irregular regions in the glomeruli's basement membrane and effacement in the podocyte pedicels. In the glomerular capillary's lumen, the endothelium nucleus and red blood corpuscles were noticed (Figure 6b).

Nanocurcumin-treated group showed a filtration barrier that appeared to be normal. It is made up of glomerular capillaries' fenestrated endothelium, a thin, uniform glomeruli's basement membrane, and numerous thin pedicels emerging from the podocyte's primary processes. In the glomerular capillary's lumen, red blood corpuscles were noticed (Figure 6c).

5. Morphometrical results: (Figure 2d, 3d, and 3h)

Statistical analysis of the mean area percentage of collagen fibers deposition, area percentage of Desmin and β -catenin immune reactions showed highly statistically significant difference rise in DEHP group comparing with other groups. On the contrary, Nanocurcumin-treated group showed a highly statistically significant decline comparing to DEHP group. However, in comparison with the control group, Nanocurcumin-treated group revealed non-significant difference.

Table 1: Mean values (\pm SD) of body weight, kidney function test (urea and creatinine), oxidative stress markers (MDA and SOD) and morphometrical analysis (area % of collagen fibers, Desmin and β -catenin immune reactions in the studied groups:

| | Control group | DEHP group | Nanocurcumin-treated group | | | |
|--|--------------------------------|-------------------------------|-----------------------------------|---------------|----------------|---|
| Groups | Mean\pm SD | Mean\pmSD | Mean\pmSD | F Test | P value | LSD |
| Body weight (gm) | 202.2 \pm 4.76 | 153.8 \pm 3.96 | 197 \pm 5.24 | 160.69 | <0.001** | 0.001**(a) 0.15 NS (b) 0.001** (c) |
| Urea (mg/dl) | 22.2 \pm 1.92 | 65 \pm 1.58 | 25 \pm 3.5 | 459.85 | <0.001** | 0.001**(a) 0.102 NS (b) 0.001** (c) |
| Creatinine (mg/dl) | 0.57 \pm 0.14 | 1.7 \pm 0.16 | 0.72 \pm 0.11 | 100.81 | <0.001** | 0.001**(a) 0.008 NS (b) 0.001** (c) |
| MDA (nmol/g) | 4.06 \pm 0.13 | 5.88 \pm 1.19 | 4.44 \pm 0.65 | 7.4 | <0.001** | 0.003*(a) 0.5 NS (b) 0.014 * (c) |
| SOD(u/mg) | 24.8 \pm 0.84 | 11.2 \pm 3.56 | 22.1 \pm 1.96 | 45.015 | <0.001** | 0.001**(a) 0.098 NS (b) 0.001** (c) |
| Mean area% collagen fibers | 1.9 \pm 0.16 | 12.99 \pm 0.74 | 2.49 \pm 0.24 | 916.91 | <0.001** | 0.001**(a) 0.06 NS (b) 0.001** (c) |
| Mean area %of Desmin | 0.64 \pm 0.08 | 14.44 \pm 2.55 | 1.76 \pm 0.69 | 126.8 | <0.001** | 0.001**(a) 0.26 NS (b) 0.001** (c) |
| Mean area% β-catenin | 3.46 \pm 1.09 | 15.33 \pm 1.4 | 5 \pm 1.5 | 116.24 | <0.001** | 0.001**(a) 0.12 NS (b) 0.001** (c) |

Values are expressed as $x \pm SD$, x: mean, Sd: Standard deviation, N=5 rats, F: ANOVA test

One way ANOVA test LSD (least significant difference), NS: Non significant ($P > 0.05$), *Significant difference ($p \text{ value} \leq 0.05$), **Highly significant difference ($p \text{ value} \leq 0.001$), (a) group 1 versus group 2, (b) group 1 versus group 3, (c) group 2 versus group 3.

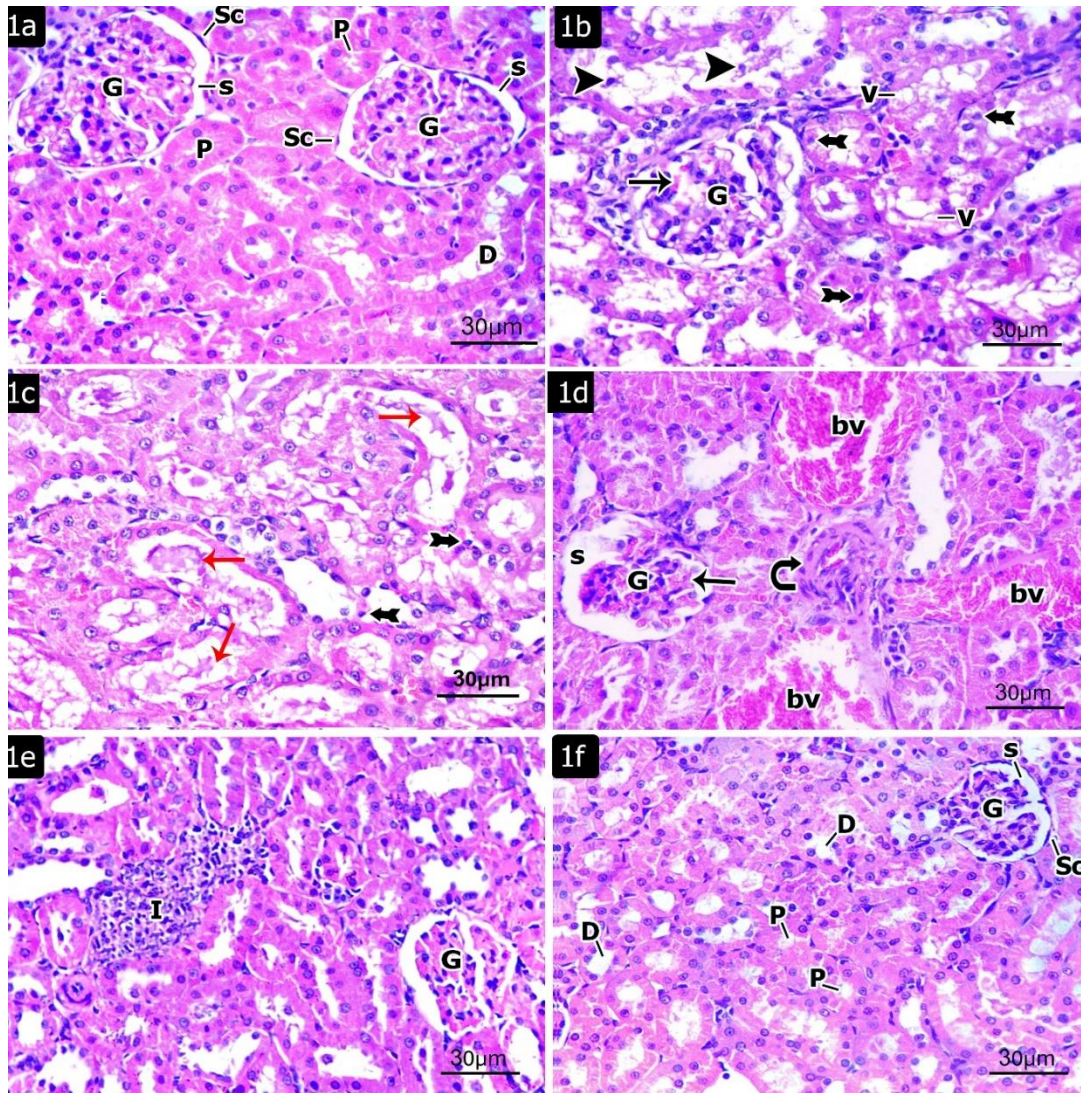


Figure (1): Photomicrograph of Hematoxylin and Eosin-stained renal cortex sections **(a) control group** revealing normal glomeruli (G) surrounded by Bowman’s space (s). Bowman’s capsule is lined with simple squamous cells (SC). The proximal (P) and distal (D) convoluted tubular cells are seen with vesicular nuclei and acidophilic cytoplasm. **(b, c, d & e) DEHP group** showing renal tubular cells with cytoplasmic vacuolation (v) and dark stained nuclei (double head arrows). Other tubules reveal desquamated epithelial cells in their lumen (arrowheads). The glomeruli (G) appears with congestion (thin arrow)**(b)**. The renal cortex showing most of tubules contain acidophilic material (red arrow) in their lumen

with dark stained nuclei (double head arrows). **(c)**. Thickened wall blood vessels (curved arrow) and congested blood vessels (bv) can be seen. Glomeruli (G) with congestion (arrow) surrounded by wide Bowman’s space (s) are also observed **(d)**. Infiltrating inflammatory cells (I) and segmented glomeruli (G) are also observed **(e)**. **(f) Nanocurcumin-treated group** showing nearly normal glomeruli (G), the capsule of Bowman is lined with simple squamous cells (SC) and the space of Bowman (s) is approximately normal. Also, proximal(P) and distal (D) convoluted tubular cells are almost normal with vesicular nuclei and acidophilic cytoplasm (**H&E X400, scale bar 30 μm**).

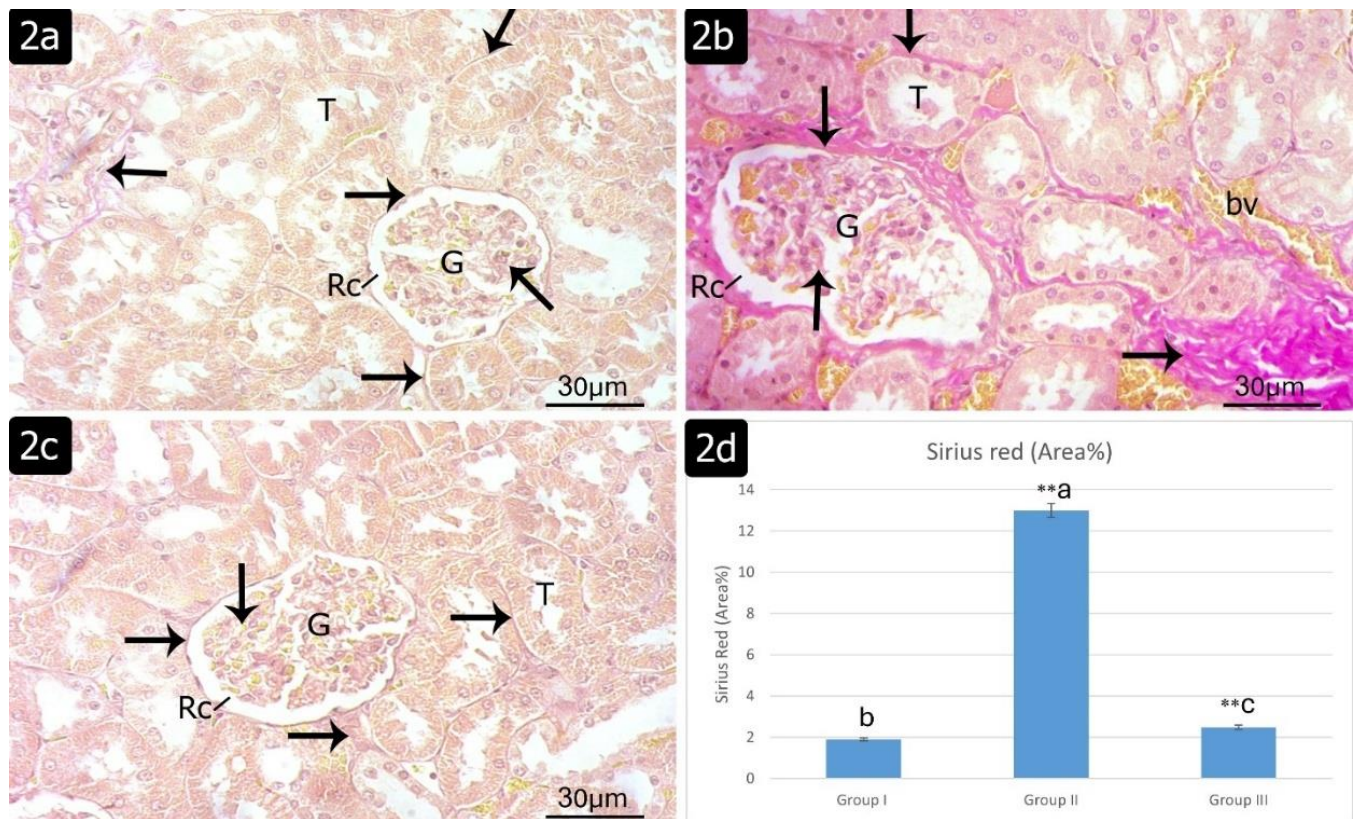


Figure 2: Photomicrograph for Sirius red stained sections from renal cortex **(a) Control group** revealing sparse collagen fibers (arrows) surrounding the kidney's tubules (T) and corpuscles (Rc) and within capillaries of glomeruli(G). **(b) DEHP group** revealing increased collagen fibers (arrows) surrounding the kidney's tubules (T) and corpuscles (Rc), within capillaries of glomeruli (G) and along the blood vessels' wall(bv). **(c)**

Nanocurcumin-treated group revealing some collagen fibers (arrows) are deposited surrounding the kidney's tubules(T) and corpuscles (Rc) and within capillaries of glomeruli(G). **(d)** Bar chart of the mean level of Sirius red (Area%) of different studied groups (**Highly significant difference (p value ≤ 0.001), (a) group 1 versus group 2, (b) group 1 versus group 3, (c) group 2 versus group 3) **(Sirius red, X 400, Scale bar 30 µm).**

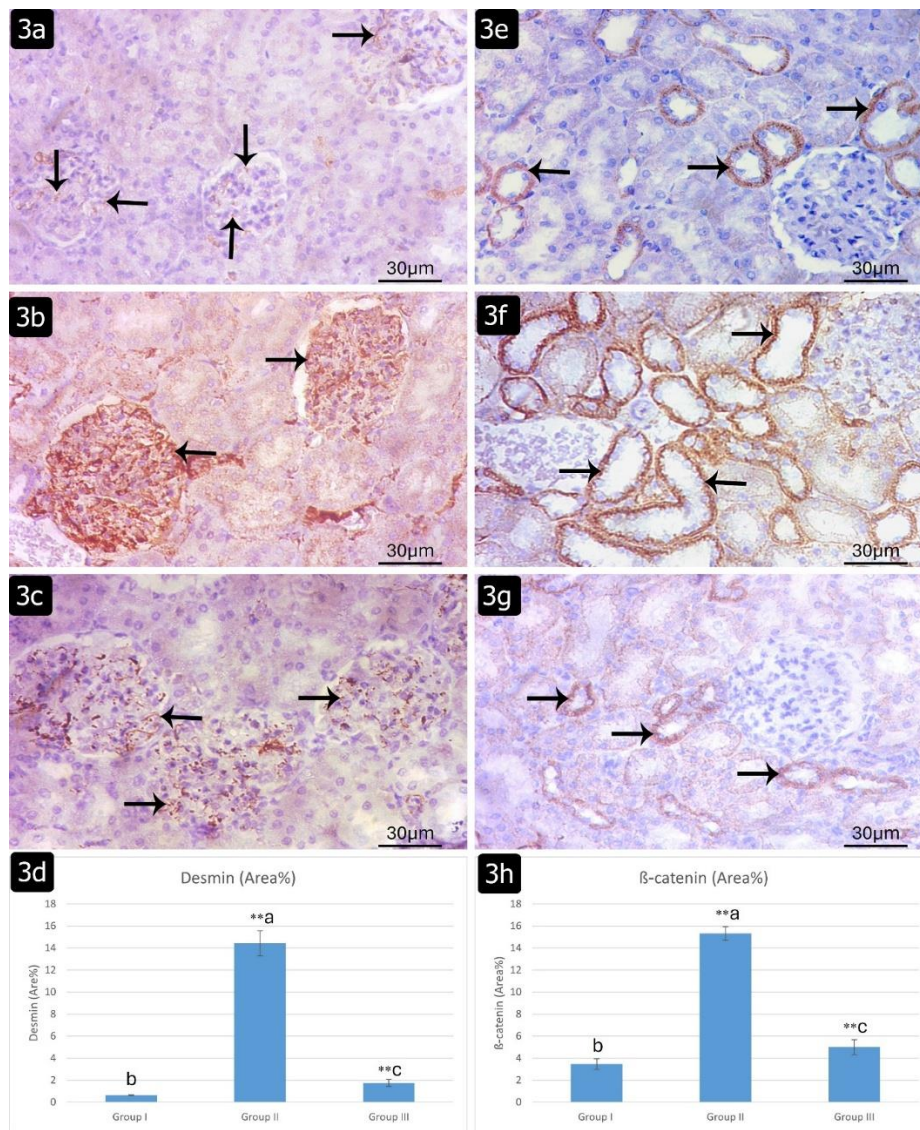


Figure 3: Photomicrograph of Desmin and β -catenin immuno stained sections from renal cortex. **(a, b, c & d) for Desmin immunoreactions:** **(a) Control group** revealing very few immunoreactions in podocyte’s cytoplasm (arrows) **(b) DEHP group** showing abundant positive brown immunoreactions in podocyte’s cytoplasm (arrows), **(c) Nanocurcumin-treated group** showing brown positive immunoreactions in some podocytes’ cytoplasm (arrows). **(d)** Bar chart of the mean level of Desmin (Area%) of different studied groups (**Highly significant difference (p value ≤ 0.001), (a) group 1 versus group 2, (b) group 1 versus group 3, (c) group 2 versus group 3). **(Immunoperoxidase for**

desmin X 400, Scale bar 30 μ m). Then **(e, f, g & h) for β -catenin immunoreactions:** **(e) Control group** showing scanty brown immunoreactions in renal tubular cells’ cytoplasm (arrows), **(f) DEHP group** reveals many positive brown immunoreactions in renal tubular cells’ cytoplasm (arrows), **(g) Nanocurcumin-treated group** showing moderately positive brown immunoreactions in renal tubular cells’ cytoplasm. **(h)** Bar chart of the mean level of β -catenin (Area%) of different studied groups (**Highly significant difference (p value ≤ 0.001), (a) group 1 versus group 2, (b) group 1 versus group 3, (c) group 2 versus group 3) **(Immunoreaction for β -catenin x400, Scale bar 30 μ m).**

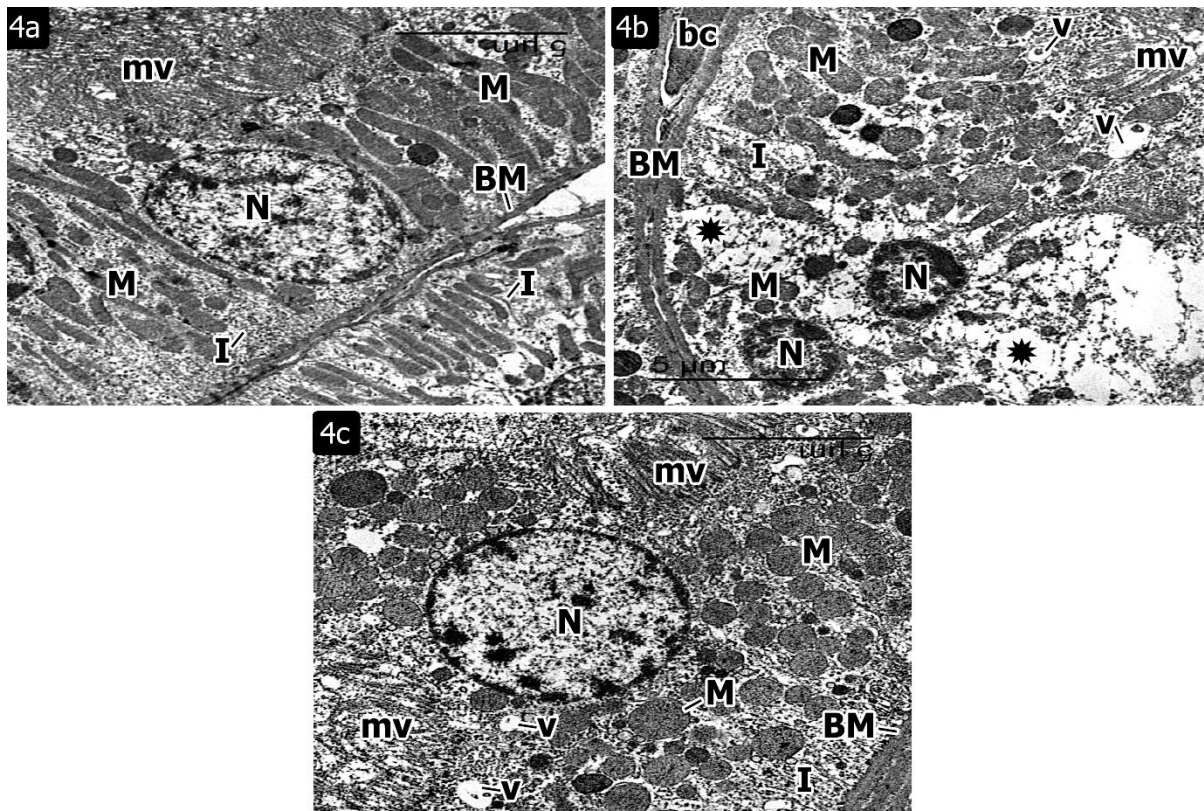


Figure (4): Electron micrographs of the proximal convoluted tubular cells :(a) **control group** revealing the proximal convoluted tubular cells rest on a thin, regular basement membrane (BM) and have regularly seen euchromatic nucleus (N) and apical microvilli (mv). The cells' basal parts reveal tightly packed parallel organized mitochondria (M) along with basal infoldings (I). (b) **DEHP group** showing a part of a proximal convoluted tubular cells with small irregular heterochromatic nuclei (N), disorganized apical microvilli (mv) and areas of rarified cytoplasm

(*) with some vacuoles (v). The cell's basal part reveals ill-organized mitochondria (M) and basal infoldings (I). Thick basement membrane (BM) and blood capillary (bc) can be seen. (c) **Nanocurcumin-treated group** showing a part of the lining epithelium of proximal convoluted tubular cell rests on thin, regular basement membrane (BM) and has regularly seen euchromatic nucleus (N) and apical microvilli(mv). The cell's basal part reveals numerous mitochondria (M) along with nearly regular basal infoldings (I). Cytoplasmic vacuoles (v) are still observed.

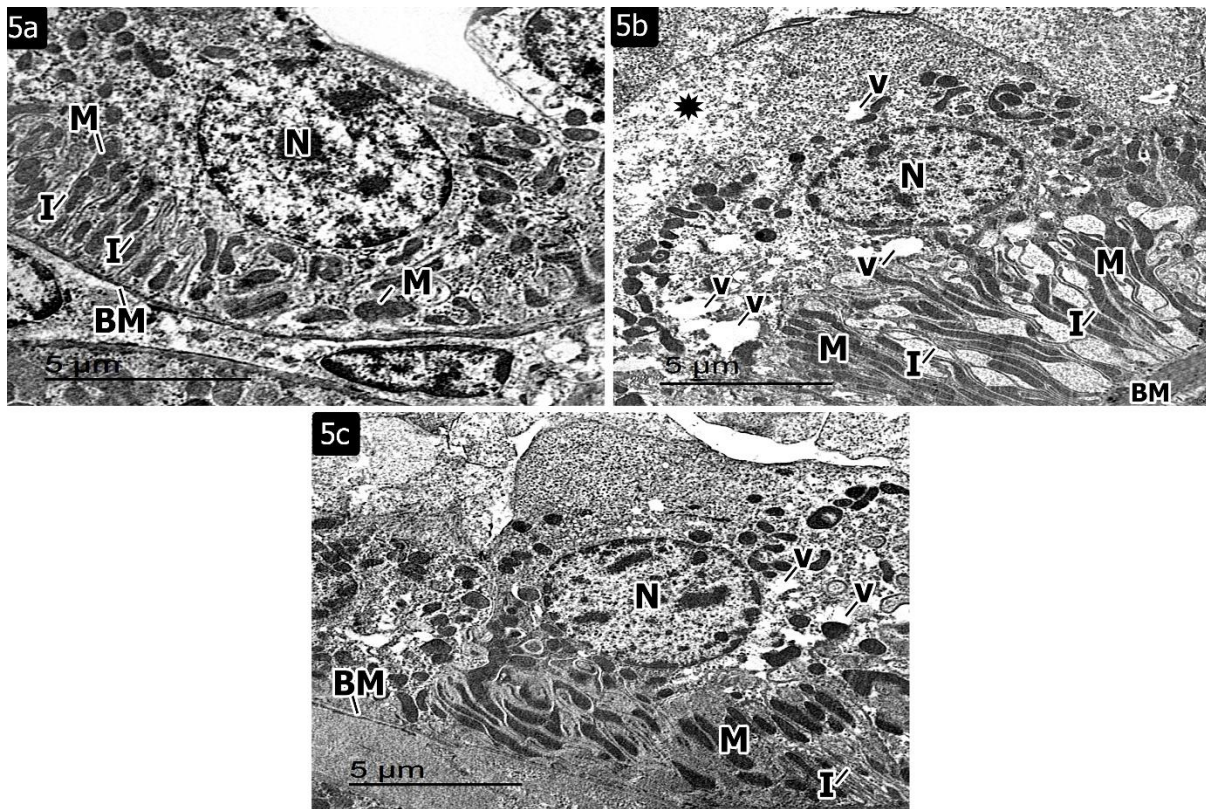


Figure 5: Electron micrographs of the distal convoluted tubular cells: **(a) Control group** revealing the distal convoluted tubular cells rest on a thin, regular basement membrane (BM) and have regularly seen euchromatic nucleus (N). The cells' basal parts reveal tightly packed parallel organized mitochondria (M) along with basal infoldings (I). **(b) DEHP group** showing a part of a distal convoluted tubular cell has euchromatic nucleus (N) and regions of rarified cytoplasm (*) with some vacuoles (v). The

cell's basal part reveals ill-organized mitochondria (M) and basal infoldings (I). Thick basement membrane (BM) can be seen. **(c) Nanocurcumin-treated group** showing a part of a distal convoluted tubular cell rests on thin, regular basement membrane (BM) and has regularly seen euchromatic nucleus (N). The cell's basal part reveals nearly organized mitochondria (M) along with nearly regular basal infoldings (I). Cytoplasmic vacuoles (v) are still observed.

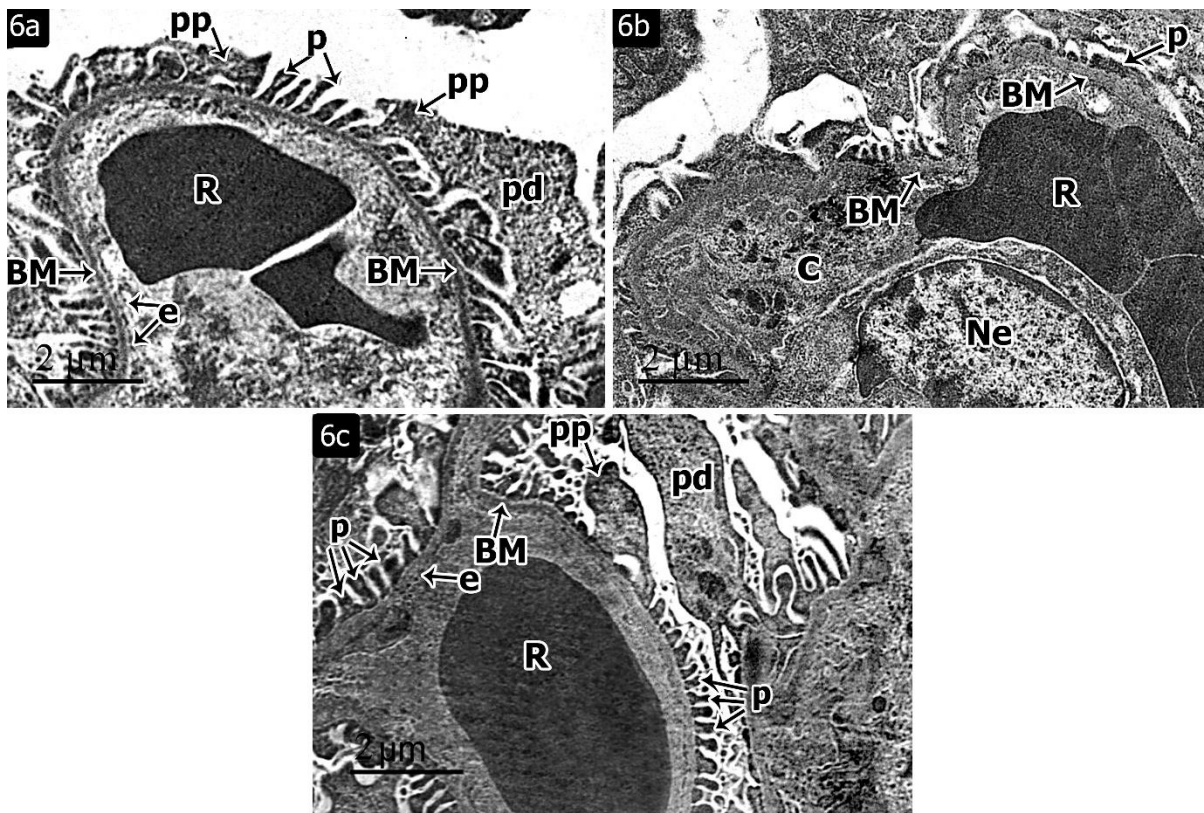


Figure 6: Electron micrographs of the blood renal barrier: (a) **Control group** revealing the primary podocyte processes (pp) that emerge from the cell body (Pd). The filtration barrier is made up of glomerular capillaries' fenestrated endothelium (e), a thin, uniform glomeruli's basement membrane (BM), and numerous thin pedicels (P). In the glomerular capillary's lumen, red blood corpuscles (R) are noticed. (b) **DEHP group** showing disruption of the filtration barrier resulting from thickened, irregular regions in the glomeruli's basement membrane (BM) and effacement in the podocyte pedicels (P). In the glomerular

capillary's lumen (c), the endothelium nucleus (Ne) and red blood corpuscles (R) are noticed. (c) **Nanocurcumin-treated group** showing a filtration barrier that appears to be normal. It is made up of glomerular capillaries' fenestrated endothelium (e), a thin, uniform glomeruli's basement membrane (BM), and numerous thin pedicels (P) emerging from the podocyte's (Pd) primary processes (pp). In the glomerular capillary's lumen, red blood corpuscles (R) are noticed.

DISCUSSION

Chronic kidney disease (CKD), predicted to affect 13.4% of the world's population, is a growing global health concern. Prevention of chronic kidney disease (CKD) is crucial because its progression to end-stage kidney failure necessitates renal replacement therapy, which creates an extensive strain on patients and the healthcare system (32, 33).

Numerous studies on both humans and animals have demonstrated that prolonged exposure to DEHP can harm renal function, cause

glomerulonephritis, and interfere with renal development (34). However, few studies were conducted to demonstrate the structural alterations of DEHP in the renal cortex. So, *the first goal* of our study was to clarify the possible histological and biochemical changes that may occur in the renal cortex of adult male albino rats after exposure to DEHP. *The second goal* was to explore the role of Nanocurcumin in counteracting the changes that occur in renal cortex as a result of exposure to DEHP. Also, it was to elucidate the mechanisms through which

Nanocurcumin induced its effects, to shed a light on the possible use of such application in the clinical field.

In the present work, no differences were observed in the general appearance, food and water intake among the rats of all groups. No mortalities were recorded. Regarding the body weight, DEHP group had a highly significant decrease impact on rat body weight when compared to other groups. This finding was in line with Caserta et al. (35) who found that there was a decrease in body weight after DEHP treatment. Also, Farag et al. (36) demonstrated that body weight is a crucial nonspecific indicator that accurately reflects the toxicity of substances and can be used to evaluate how DEHP affects rat growth.

Moreover, Zhou et al. (37) postulated that DEHP forces mice to eat less, which lowers their body weight. It can also cause multi-organ stress, which is the body's stress reaction to DEHP's toxicity.

In this study, Nanocurcumin-treated group revealed enhancement of rats overall circumstances provoked via significant increase in body weight versus DEHP group. This finding agreed with El-Desoky et al. (38) who found rise in body weight gain and proposed that food metabolism and digestion are improved when nanocurcumin is taken in because it increases antioxidant capacity or scavenges free radicals.

In the present work, statistical analysis of mean serum levels of urea and creatinine demonstrated high significant rise in DEHP group comparing to control and Nanocurcumin-treated groups. Similar findings were mentioned by Amara et al. (39) who examined how oxidative stress was linked to changes in serum creatinine, urea, and lactate dehydrogenase levels, which are indicators of renal damage. In fact, this phthalate's effect on cell homeostasis is reflected in the rise in these levels.

On the contrary, statistical analysis of mean serum levels of urea and creatinine showed highly significant drop in the Nanocurcumin-treated group versus DEHP group. El-Gizawy

et al. (40) revealed the capability of Nanocurcumin to preserve the kidney function, demonstrated by normal levels of biomarkers for kidney function tests, and its effectiveness in reducing lipid peroxidation because it directly scavenges free radicals and strengthens antioxidant defenses.

Liguori et al. and Amara et al. (39, 41) stated that the imbalance between the generation of free radicals and the antioxidants' ability to neutralize them is known as oxidative stress. It is suggested that phthalates' induction of oxidative stress is an important aspect in DEHP toxicity. Furthermore, Ashari et al. (42) documented that one of the processes that contributes to DEHP-induced nephrotoxicity is oxidative stress. ROS concentrations got higher, which can harm cell macromolecules like proteins, lipids, and DNA.

MDA, an oxidative marker, is the lipid peroxidation's final product and the rise of its production within kidney tissues demonstrating increased tissue and cell damage. In our work, statistical analysis of MDA mean values setup an evidence of cell injury by revealing a significant rise in the DEHP group when compared to the other groups. This result agreed with Li et al. (43).

Islam et al. (44) established that SOD was an active ingredient that could get rid of toxic substances from an organism's metabolism. In order to shield cells from oxidative damage, SOD scavenges oxygen free radicals. Oxidative stress in our work was also confirmed by high significant decline in SOD mean values in the DEHP group compared to other groups. In addition, Akinwumi, (45) clarified that oxidative stress caused by DEHP was evidenced by increased MDA and decreased SOD levels, which resulted in an accumulation of lipids and possible cell death.

In the Nanocurcumin-treated group, MDA level demonstrated significant decline, while SOD level revealed highly significant rise compared to DEHP group. This finding coincided with Tohamy et al. (46) who stated that Nanocurcumin minimized hepatorenal toxicity by preserving the status of antioxidant enzymes

like SOD and reducing lipid peroxidation by inducing enzymatic and non-enzymatic antioxidants and lowering inflammatory mediators.

DEHP induced renal cortical alternations that were confirmed by light and electron microscopes. Our findings were confirmed by Shen et al. (21) who found that DEHP modifies the body's oxidative stress level and causes pathological damage. Excess free radicals damage cell membranes and increase their permeability, which ultimately results in oxidative damage.

In the current work, DEHP group showed some tubular epithelial cells with small darkly stained nuclei and numerous cytoplasmic vacuolations. This was in agreement with Aydemir et al. and Li et al. (43, 47). Soliman et al. (48) explained that the renal tubule's epithelial cells were highly active ion transporters with electro-charged surfaces, making them extremely vulnerable to toxic injury because they absorbed and concentrated toxins. Additionally, Ahmad and Ameen, and Mahmoud et al. (49, 50) proposed that cellular vacuolation may serve as a defense mechanism for harmful substances. These compounds were kept apart in vacuoles so they wouldn't interfere with the metabolism of cells. This alteration represents one of the initial response mechanisms to each kind of cellular damage, where an increase in cell membrane permeability causes water to accumulate inside the cells.

Other renal tubules in DEHP group in our study revealed desquamated epithelial cells in their lumen. Abdel-Kawi et al. and Han et al. (51, 52) found similar changes and assumed that following DEHP exposure in a testicular model, the cell junction might be more vulnerable to damage. Ola-Davies et al. (53) added that cell debris and exfoliated cells in the renal tubules suggested a decline in the kidneys' proximal and distal convoluted tubules' capacity to absorb substances.

Moreover, in the current work, most tubules are distorted and contained acidophilic materials in their lumen. This was agreed with Al-Qahtani et al. (54) who attributed this to the fact that

oxidative stress causes lipid peroxidation to rise, which damages cellular membranes.

The protein and lipid components of intracellular membranes are destroyed by lipid peroxidation and free radical production, which also hydrolyzes the cytoplasm. Tubular cells contribute to the formation of casts when they shed into the lumen of tubules. The casts cause ultrafiltrate to flow back across the tubular basement membrane by blocking the tubular lumen and raising intratubular pressure (55).

In the present work, DEHP- group revealed lost, shrunken and segmented glomeruli. This glomerular atrophy was also reported by Gad El-Karim et al. (56). Omorodion et al. (57) explained this by the excessive strain on the kidneys as they try to filter and channel off harmful metabolites after DEHP is broken down into smaller molecules. Also, Ahmad and Ameen (49) hypothesized that glomerular shrinkage may result from tubular injury's ability to reduce the glomerular filtration rate. Renal vasoconstriction in reaction to various nephrotoxic substances was the explanation for these changes, which included segmented or shrunken glomeruli. Oxidative stress was also thought to be the cause of some glomeruli's shrinkage (58).

Vascular congestion of some glomeruli and blood vessels were noticed in DEHP group. Akinwumi, and Ashari et al. (45, 59) explained this by endothelial damage due to oxidative stress mediated by ROS. Also, Abdelrahman et al. (60) attributes these alterations on nitric oxide overproduction that makes damages to cells' proteins, lipids, and DNA ultimately leads to cell death. Saleh et al. (61) stated that NO is a potent vasodilator that increases blood flow and congestion.

The reason for the thickening of the blood vessel wall is that stress can cause the release of several vasoactive substances, including nitric oxide and endothelin (ET-1), which encourages the growth of vascular smooth muscle cells and endothelial cells (49).

DEHP group also showed infiltration of inflammatory cells. One important pathophysiological pathway for DEHP-induced

neurotoxicity is thought to be inflammation. DEHP can disrupt cellular respiration, impact mitochondrial function, and raise pro-inflammatory cytokine production, all of which can result in cell death. Furthermore, DEHP-induced inflammation was linked to classical innate immune system activation through toll-like receptor (TLR4) activation (62, 63). More recently, Al-Qahtani et al. (54) reported that DEHP increased monocytes' or macrophages' production of TNF- α . TNF- α is a vital pro-inflammatory cytokine that is mostly released by monocytes and macrophages. It is crucial in prompting local and systemic inflammation by inducing other cytokines, such as IL-1 β and IL-6. This could explain infiltrating inflammatory cells seen in our study.

Electron microscopic examination of the same group demonstrated the tubular cells with rarified cytoplasm. Saleh et al. and Li et al. (61, 64) explained the previous finding to the lysosomal membrane damage which brought on by dangerous drugs. As a consequence of the spillover of their potent enzymes and vulnerability to pathologic effects, these membranes are destroyed, which causes different cellular components to dissolve and degenerate.

Moreover, ultrastructural examination of DEHP group the renal cortex showed disruption of the filtration barrier resulting from thickened, irregular regions in the glomeruli's basement membrane and effacement in the podocyte pedicels. El-haleem et al. (65) clarified that interference with structural elements of the slit diaphragm, the actin cytoskeleton, or the podocyte-glomerular basement membrane interaction are the causes of the podocytes' effacement of the foot processes. Additionally, Increased glycoprotein deposition might be linked to irregular thickening of the tubular and glomerular basement membrane. Moreover, these results were explained by Ahmad and Ameen (49), who attributed these modifications to direct damage to the podocyte skeleton following ROS exposure, or they might arise as a result of the glomerular basement membrane thickening to make up for increased glomerular

permeability and proteinuria. Ali et al. (66) claimed that the large surface area of the glomerular capillaries, which are susceptible to high levels of toxins and immunological complexes in the blood, may be the cause of the irregular glomerular basement membrane thickening.

Isaac (67) established that glomerular damage and tubular interstitial injury are related, as podocyte damage causes significant plasma protein leakage into the tubules. Following their reabsorption by the PCT, mediators such as endothelin, platelet-derived growth factor, and monocyte chemoattractant protein type 1 were secreted into the interstitium. These mediators cause an inflammatory response that result in tubular degeneration and interstitial fibrosis.

Increased collagen fiber deposition in the DEHP group is a predictable result of the previously reported results. In this work, examination of Sirius red stained-sections showed abundant aggregations of collagen fibers. This was confirmed by morphometrical analysis. Increased fibrosis was the outcome of the interaction between fibroblasts and inflammatory cells. Witherel et al. (68) outlined how the interaction between macrophages and fibroblasts promotes fibrosis considering macrophages release inflammatory cytokines like IL-6, IL1-B, TNF α , and TGFB, that promote fibroblast differentiation and proliferation to myofibroblasts with increased collagen fiber aggregations.

Fibrosis is caused by an imbalance in extracellular matrix formation and breakdown, epithelial-to-mesenchymal transition, and fibroblast stimulation. Together with local and circulating cells, the primary mechanism of renal fibrosis is the epithelial to mesenchymal transition (EMT), a process in which tubular epithelial cells change into mesenchymal fibroblasts that migrate to adjacent interstitial parenchyma. Excessive extracellular matrix collagen deposition was linked to interstitial fibroblasts, which exert excess extracellular matrix (ECM), and defective collagen-synthesizing epithelial cells, which manifest as interstitial fibrosis and thickening of the

basement membrane (69, 70). Similar results were reported by Shi et al. (71), they revealed that DEHP exposure could lead to epithelial-interstitial transformation and renal fibrosis progression in renal tubular cells.

The intermediate filament protein desmin is only weakly expressed in healthy glomerular podocytes. The main elements of the renal filtration barrier are the glomerular podocytes. The function of desmin is to increase the cells' mechanical resistance. Its increased expression in podocytes indicates morphological changes brought on by injury (72).

In the present study, regarding to desmin immunolocalization, there was highly statistical significant rise of area % of desmin in DEHP group comparing to control and Nanocurcumin-treated groups. El-Mahalaway (73) claimed that the induction of mesenchymal markers like desmin coincided with podocyte epithelial dedifferentiation. It was postulated that podocytes could undergo mesenchymal transition and epithelial dedifferentiation as a result of elevated transforming growth factor- β 1 (TGF- β 1) in kidney disease. They added that podocytes' de novo desmin expression may serve as a trustworthy and pertinent indicator of the podocyte epithelial-to-mesenchymal transition. Moreover, Huang et al. (74) reported that TGF- β 1 increases the expression of desmin and caspase 9, which leads to apoptosis. Also, Fadda et al. (75) stated that podocytes are unable to be replaced once they are lost due to their limited capacity for division and repair, which leads to structural cell damage and increased filtration barrier leakage, ultimately leading to chronic kidney disease. Desmin staining is a sensitive indicator of very early podocyte damage as a result.

Numerous physiological, pathological, and developmental processes in the kidney are linked to the intracellular molecule β -catenin, which is involved in cell adhesion, cell signaling, and gene transcription regulation. After binding to E-cadherin at the cell membrane, β -Catenin can stabilize the cell adhesion junction. Wnt signaling, which controls the expression of genes linked to cell

differentiation and proliferation, is also mediated by β -catenin (76, 77).

In the current work, β -catenin immune reaction showed a highly statistical significant increase of area % of β -catenin in DEHP- group as compared with other groups. Üstündağ et al. (78) postulated that EDCs are thought to be hazardous even at sub-nanomolar concentrations due to their strong affinity for binding to membrane receptors. Therefore, through altered intracellular β -catenin levels, EDCs can influence tumorigenesis, cancer, apoptosis, cell proliferation, and the epithelial-to-mesenchymal transition. Similar results were mentioned by Hu et al. (79), they postulated that DEHP can inhibit cellular adhesion, differentiation, promote autophagy and apoptosis by affecting the stability and transcriptional activity of β -catenin. DEHP activates the Wnt signaling pathway resulting in increased the expression of β -catenin.

In the present study, histological examination of the renal cortex of Nanocurcumin-treated group revealed almost normal histological architecture. These findings agreed with El-Gizawy et al. and Tohamy et al. (40, 46) who stated that Nanocurcumin mitigated the hepatorenal toxicity through amelioration of the histological injury and its antioxidant properties also guard against the production of ROS. Nanocurcumin's main chemotherapeutic effectiveness is dependent on its ability to modulate inflammatory responses, antioxidants, and free-radical defense mechanisms. Because of its anti-inflammatory properties, nanocurcumin suppresses TNF- α by inactivating the nuclear transcription factor kappa B and inhibiting the expression of the TNF- α gene.

Ultrastructural findings were coincided with these light observations. From these results, Nanocurcumin-treated group showed that the renal cortex's structural and ultra-structural modifications were mainly restored. These findings were in line with Şener Akçora et al. (80) who demonstrated that curcumin has been shown to aid in the restoring glomerular and tubular structures in kidney injury mediated by

its anti-inflammatory and antioxidant properties. Furthermore, Bayoumi et al. and El Shahawy and El Deeb, (19, 81) provided an evidence of the potent curative effect of Nanocurcumin in alleviation of histopathological and ultrastructural alterations in the lung and submandibular gland respectively pointing out its anti-oxidant properties.

In this work, examination of Sirius red stained sections of Nanocurcumin-treated group revealed decreased collagen fibers around tubules and glomeruli. It was confirmed by morphometrical and statistical analysis which showed highly significant decline in area percentage of collagen fibers in Nanocurcumin-treated group versus DEHP-treated group. Similar results were obtained by Guo et al. and Embaby and Abdel-Kawi (82, 83), who mentioned that curcumin reduced collagen deposition in the liver and attributed that to downregulation of transforming growth factor 1 (TGF- β 1). Moreover, Atia et al. (84) observed the decrease of testis fibrosis after treatment with curcumin and Nanocurcumin and referred this to the antioxidant mechanism of them which was in charge of preserving the activity of antioxidant enzymes and capturing free radicals. In addition, this finding coincided with Elmasry and Bondok (85), who demonstrated that curcumin has been shown to aid in the resolution of renal fibrosis during the priming and activation stages by limiting inflammation, restoring redox balance, suppressing EMT, and removing ECM excess deposition.

Regarding to desmin immune reaction in the present study, there was highly statistical significant decline in area percentage of desmin in Nanocurcumin-treated group versus DEHP group. Similar findings were correlated with El-Mahalaway (73), who attributed that curcumin's potent anti-inflammatory and antioxidant properties provided a kidney-protective effect. According to this finding, one of the main

mechanisms regulating injured podocytes is the reduction in desmin protein expression.

In the current work, there was highly statistically significant decrease in area percentage of β -catenin in Nanocurcumin-treated group versus DEHP group. Ambacher et al. and Tao et al. (86, 87) attributed that the canonical WNT/ β -catenin pathway is rendered inactive by a number of WNT inhibitors. The primary inhibitor of the WNT pathway is Glycogen Synthase Kinase 3 β (GSK-3 β). GSK-3 β is an intracellular serine-threonine kinase that is specific to neurons and controls a number of signaling pathways, including cell membrane signaling, inflammation, and neuronal polarity. Nuclear migration and β -catenin cytosolic stabilization are inhibited by GSK-3 β . Furthermore, Vallée et al. (88) suggested that curcumin enhances GSK-3 β activity, which lowers the level of nuclear β -catenin. In summary, curcumin stimulates GSK-3 β activity by decreasing the WNT pathway, which causes β -catenin to become phosphorylated and subsequently degrade.

CONCLUSIONS

Nanocurcumin's anti-inflammatory and anti-apoptotic properties help to mitigate renal cortical damage caused by DEHP. Thus, this may create a new treatment option for human DEHP toxicity.

Recommendation In order to comprehend how DEHP may impact the physiology of various tissues, more research is required to examine the molecular basis of these changes. To determine the long-term efficacy of nanocurcumin, more research should be done.

Declaration of interest

The authors report no conflicts of interest. The authors along are responsible for the content and writing of the paper.

Funding information

None declared

REFERENCES

- Kahn LG, Philippat C, Nakayama S F, Slama R, Trasande L. Endocrine-disrupting chemicals: implications for human health. *The lancet Diabetes & endocrinology*. (2020); 8(8), 703-18.
- Laws M J, Neff A M, Brehm E, Warner G R, Flaws J A. Endocrine disrupting chemicals and reproductive disorders in women, men, and animal models. In *Advances in pharmacology*. Academic Press. (2021); (Vol. 92, pp. 151- 90).
- Walker C, Garza S, Papadopoulos V, Culty M. Impact of endocrine-disrupting chemicals on steroidogenesis and consequences on testicular function. *Molecular and Cellular Endocrinology*. (2021); 527, 1-10.
- Sherif N A E H, El-Banna A, Abdel-Moneim R A, Sobh Z K, Balah M I F. The possible thyroid disruptive effect of di-(2-ethyl hexyl) phthalate and the potential protective role of selenium and curcumin nanoparticles: A toxicological and histological study. *Toxicology Research*. (2022); 11(1), 108-21.
- Robles-Matos N, Radaelli E, Simmons R A, Bartolomei M S. Preconception and developmental DEHP exposure alter liver metabolism in a sex-dependent manner in adult mouse offspring. *Toxicology*. (2023); 499, 1-3.
- Günaydin N, Altin E, Ormanci N, Ertekin A. The Effect of Di (2-Ethylhexyl) Phthalate on Hair Trace Mineral Levels in Rats. *Biological Trace Element Research*. (2022); 9, 1-5.
- Liu Y, Guo Z, Zhu R, Gou D, Jia P P, Pei D S. An insight into sex-specific neurotoxicity and molecular mechanisms of DEHP: a critical review. *Environmental Pollution*. (2023); 316, 1-14.
- Interdonato L, Siracusa R, Fusco R, Cuzzocrea S, Di Paola R. Endocrine disruptor compounds in environment: Focus on women's reproductive health and endometriosis. *International Journal of Molecular Sciences*. (2023); 24(6), 1-5.
- Chen Y, Wang Y, Xu Y, Sun J, Yang L, Feng C, Wang, Y. Molecular insights into the catalytic mechanism of plasticizer degradation by a monoalkyl phthalate hydrolase. *Communications Chemistry*. (2023); 6(1), 40-5.
- Su H Y, Lai C S, Lee, K H, Chiang YW, Chen C C, Hsu P C. Prenatal exposure to low-dose di-(2-ethylhexyl) phthalate (DEHP) induces potentially hepatic lipid accumulation and fibrotic changes in rat offspring. *Ecotoxicology and Environmental Safety*, (2024); 269, 1-9.
- Nayak S R R, Boopathi S, Haridevamuthu B, Arockiaraj J. Toxic ties: Unraveling the complex relationship between endocrine disrupting chemicals and chronic kidney disease. *Environmental Pollution*. (2023); 338, 1-4.
- Khan I, Saeed K, Khan I. Nanoparticles: Properties, applications and toxicities. *Arabian journal of chemistry*. (2019); 12(7), 908-31.
- Chandrakala V, Aruna V, Angajala, G. Review on metal nanoparticles as nanocarriers: Current challenges and perspectives in drug delivery systems. *Emergent Materials*. (2022); 5(6), 1593-615.
- Rahman F, Sarma J, Mohan P, Barua C C, Nath R, Rahman S, Sarma M. Role of Nano-curcumin on carbon tetrachloride (CCl₄) induced hepatotoxicity in rats. *Journal of Pharmacognosy and Phytochemistry*. (2020); 9(2), 2168-76.
- Karthikeyan A, Senthil N, Min T. Nanocurcumin: A promising candidate for therapeutic applications. *Frontiers in Pharmacology*. (2020); 11, 487-98.
- Ali M F, Sadek A S, Abd Elghfar S K, Taha M. Nano-curcumin Attenuates Nephropathic Lesions Induced by Chronic Ketoprofen Administration in Rats: Role of Cyclooxygenase-1. *Journal of Advanced Veterinary Research*. (2022); 12(5), 524-34.
- Hosseinzadeh A, Mehrzadi S, Siahpoosh A, Basir Z, Bahrami N, Goudarzi M. Gallic acid ameliorates di-(2-ethylhexyl) phthalate-induced testicular injury in adult mice. *Human & Experimental Toxicology* (2022); 41, 1-11.
- Shamsi-Goushki A, Mortazavi Z, Mirshekar M A, Mohammadi M, Moradi-Kor N, Jafari-Maskouni S, Shahraki M. Comparative effects of curcumin versus nano-curcumin on insulin resistance, serum levels of apelin and lipid profile in type 2 diabetic rats. *Diabetes, Metabolic Syndrome and Obesity*. (2020); 2337-46.
- El Shahawy M, El Deeb M. Assessment of the possible ameliorative effect of curcumin nanoformulation on the submandibular salivary gland of alloxan-induced diabetes in a rat model (Light microscopic and ultrastructural study). *The Saudi Dental Journal*. (2022); 34(5), 375-84.
- Salah A, Yousef M, Kamel M, Hussein A. The neuroprotective and antioxidant effects of Nanocurcumin oral suspension against lipopolysaccharide-induced cortical neurotoxicity in rats. *Biomedicines*. (2022); 10(12), 3087-95.
- Shen Y, Liu L, Li M Z, Wang H R, Zhao Y, Li J L. Lycopene prevents Di-(2-ethylhexyl) phthalate-induced mitophagy and oxidative stress in mice heart via modulating mitochondrial homeostasis. *The Journal of Nutritional Biochemistry*. (2023); 115, 1-9.
- Abdel-Halim K Y, Osman S R, Abuzeid M A F, Khozimy A. M. Hematological Changes and Oxidative Stress Induction of Titanium Dioxide Nanoparticles in Male Mice after Intraperitoneal Injection of Different Doses for 28 Days: Study of Organ's Responsibility. *NanoWorld J*. (2021); 7(2), 22-32.
- Odukoya O, Sofidiya M, Ilori O, Gbededo M,

- Ajadotuigwe J, Olaleye O, Brinkhaus B. Malondialdehyde determination as index of lipid peroxidation. *Int. J. Biol. Chem.* (1994); 3, 281-85.
24. Weydert C J, Cullen J J. Measurement of superoxide dismutase, catalase and glutathione peroxidase in cultured cells and tissue. *Nature protocols*; (2010); 5(1), 51-66.
 25. Odukoya O, Sofidiya M, Ilori O, Gbededo M, Ajadotuigwe J, Olaleye O, ... & Brinkhaus B. Malondialdehyde determination as index of lipid peroxidation. *Int. J. Biol. Chem.* (1994); 3, 281-5.
 26. Weydert C J. & Cullen J J. Measurement of superoxide dismutase, catalase and glutathione peroxidase in cultured cells and tissue. *Nature protocols*, (2010); 5(1), 51-66.
 27. Bazzano T, Restel T I, Porfirio L C, Souza A S D, & Silva I S. Renal biomarker of male and female Wistar rats (*Rattus norvegicus*) undergoing renal ischemia and reperfusion. *Acta cirurgica brasileira*, (2015); 30(4), 277-88.
 28. Suvarna K S, Layton C, Bancroft J D. Bancroft's theory and practice of histological techniques. Elsevier health sciences. 8th ed. (2018); 337- 95.
 29. Ramos-Vara J A, Kiupel M, Baszler T, Bliven L, Brodersen B, Chelack B, Valli V E. Suggested guidelines for immunohistochemical techniques in veterinary diagnostic laboratories. *Journal of veterinary diagnostic investigation.* (2008); 20(4), 393-413.
 30. Tizro P, Choi C, & Khanlou N. Sample preparation for transmission electron microscopy. *Biobanking: methods and protocols*; (2018); 417-424.
 31. Dean A, Dean G, Colombier D. Epi-info version 1 for the year 2000 Date Basic Statics and Epidemiology on Microcomputer CDC. Georgia, USA. (2000); 5 (10), 81-89.
 32. Hill N R, Fatoba S T, Oke J L, Hirst J A, O'Callaghan C A, Lasserson D S, Hobbs F R. Global prevalence of chronic kidney disease—a systematic review and meta-analysis. *PloS one.* (2016); 11(7), 1-18.
 33. Kang H, Kim S, Lee G, Lee I, Lee J P, Lee J, Choi K. Urinary metabolites of dibutyl phthalate and benzophenone-3 are potential chemical risk factors of chronic kidney function markers among healthy women. *Environment international.* (2019); 124, 354-60.
 34. Li M Z, Zhao Y, Wang H R, Talukder M, Li J L. Lycopene preventing DEHP-induced renal cell damage is targeted by aryl hydrocarbon receptor. *Journal of agricultural and food chemistry.* (2021); 69(43), 12853-61.
 35. Caserta D, Costanzi F, De Marco M P, Di Benedetto L, Matteucci E, Assorgi C, Ruscito, I. Effects of endocrine-disrupting chemicals on endometrial receptivity and embryo implantation: a systematic review of 34 mouse model studies. *International Journal of Environmental Research and Public Health.* (2021); 18(13), 6840-65.
 36. Farag A, FARUK E, KHARBOUSH T, Abu-Raia N H. Protective effect of N-acetylcysteine (NAC) against Di-ethylhexyl phthalate (DEHP) induced pulmonary toxicity in male albino rats (histological and immunohistochemical study). *The Egyptian Journal of Forensic Sciences and Applied Toxicology.* (2021); 21(2), 89-109.
 37. Zhou X, Zhang Z, Shi H, Liu Q, Chang Y, Feng W, Sun S. Effects of Lycium barbarum glycopeptide on renal and testicular injury induced by di (2-ethylhexyl) phthalate. *Cell Stress and Chaperones.* (2022); 27(3), 257-71.
 38. El-Desoky G E, Wabaidur S M, AlOthman Z A, Habila M A. Evaluation of Nano-curcumin effects against Tartrazine-induced abnormalities in liver and kidney histology and other biochemical parameters. *Food Science & Nutrition.* (2022); 10(5), 1344-56.
 39. Amara I, Salah A, Timoumi R, Annabi E, Scuto M, Trovato A, Abid-Essefi S. Effect of di (2-ethylhexyl) phthalate on Nrf2-regulated glutathione homeostasis in mouse kidney. *Cell Stress and Chaperones.* (2020); 25(6), 919-28.
 40. El-Gizawy M M, Hosny E N, Mourad H H, Abd-El Razik A N. Curcumin nanoparticles ameliorate hepatotoxicity and nephrotoxicity induced by cisplatin in rats. *Naunyn-Schmiedeberg's Archives of Pharmacology.* (2020); 393, 1941-53.
 41. Liguori I, Russo G, Curcio F, Bulli G, Aran L, Della-Morte D, Abete P. Oxidative stress, aging, and diseases. *Clinical interventions in aging.* (2018); 26(13), 757-72.
 42. Ashari S, Karami M, Shokrzadeh M, Bagheri A, Ghandadi M, Ranaee M, Mohammadi H. Quercetin ameliorates Di (2-ethylhexyl) phthalate-induced nephrotoxicity by inhibiting NF-κB signaling pathway. *Toxicology Research.* (2022); 11(2), 272-85.
 43. Li M Z, Zhao Y, Dai X Y, Talukder M, Li J L. Lycopene ameliorates DEHP exposure-induced renal pyroptosis through the Nrf2/Keap-1/NLRP3/Caspase-1 axis. *The Journal of Nutritional Biochemistry.* (2023); 113, 1-9.
 44. Islam M N, Rauf A, Fahad F I, Emran T B, Mitra S, Olatunde A, ... & Mubarak M S. Superoxide dismutase: an updated review on its health benefits and industrial applications. *Critical Reviews in Food Science and Nutrition.* (2022); 62(26), 7282-7300.
 45. Akinwumi, K. A. Vitamin E Alleviates Diethylhexyl Phthalate-Induced Haemato-logical Changes and Splenic Oxidative Injury in Male Sprague-Dawley Rats. *Journal of Cancer Research Updates.* (2019); 8(1), 42-51.
 46. Tohamy H G, El Okle O S, Goma A A, Abdel-Daim M M, Shukry M. Hepatorenal protective effect of nano-curcumin against nano-copper oxide-mediated toxicity in rats: Behavioral performance, antioxidant,

- anti-inflammatory, apoptosis, and histopathology. *Life Sciences*. (2022); 292, 1-12.
47. Aydemir D, Karabulut G, Şimşek G, Gok M, Barlas N, Ulusu N N. Impact of the di (2-ethylhexyl) phthalate administration on trace element and mineral levels in relation of kidney and liver damage in rats. *Biological trace element research*. (2018); 186, 474-88.
 48. Soliman M, El-Sharkawy R, Soliman M, Elsaify G. Ameliorative effects of dates on induced toxicity of aflatoxin B1 on the renal cortex of adult male albino rats: histological, immunohistochemical and biochemical study. *Journal of Medical Histology*. (2020); 4(2), 133- 61.
 49. Ahmad M M, & Ameen S H. Histopathological Changes Produced by Bisphenol A in the Renal Cortex of Adult Male Albino Rats. *The Medical Journal of Cairo University*. (2019); 87, 2045-58.
 50. Mahmoud A A E D, Seliem A O, Selim S A, Ibrahim N E. The sensitivity of adult male albino rat prostate to low-dose bisphenol A: a histological and immunohistochemical study. *Zagazig University Medical Journal*. (2024); 30(1), 250-58.
 51. Abdel-Kawi S H, Hashem K S, Abd-Allah S. Mechanism of diethylhexylphthalate (DEHP) induced testicular damage and of grape seed extract-induced protection in the rat. *Food and Chemical Toxicology*. (2016); 90, 64-75.
 52. Han L, Wang J, Zhao T, Wu Y, Wei Y, Chen J, Wei G. Stereological analysis and transcriptome profiling of testicular injury induced by di-(2-ethylhexyl) phthalate in prepubertal rats. *Ecotoxicology and Environmental Safety*. (2021); 220, 1-11.
 53. Ola-Davies E O, Olukole S G, Lanipekun D O. Gallic acid ameliorates bisphenol a-induced toxicity in Wistar rats. *Iranian Journal of Toxicology*. (2018); 12(4), 11-18.
 54. Al-Qahtani M A, Virk P, Awad M, Elobeid M, Alotaibi K S. Attenuation of di (2-ethylhexyl) phthalate-induced hepatic and renal toxicity by naringin nanoparticles in a rat model. *Green Processing and Synthesis*. (2023); 12(1), 1-14.
 55. El-sherif N M, Issa N M. Protective effect of rosemary (*Rosmarinus officinalis*) extract on naphthalene induced nephrotoxicity in adult male albino rat. *J Interdiscip Histopathol*. (2015); 3(1), 24-32.
 56. Gad El-Karim D R, Lebda M A, Alotaibi B S, El-Kott A F, Ghamry H I, Shukry M. Lutein modulates oxidative stress, inflammatory and apoptotic biomarkers related to di-(2-ethylhexyl) phthalate (dehp) hepato-nephrotoxicity in male rats: role of nuclear factor kappa b. *Toxics*, (2023); 11(9), 740-9.
 57. Omorodion N T, Atoigwe-Ogeyemhe B E, Achukwu P U, Odigie E B. Histopathological changes associated with exposure of some viscerals and testicular tissues to bisphenol A and di (2-ethylhexyl) phthalate. *Tropical Journal of Pharmaceutical Research*. (2019); 18(6), 1213-18.
 58. Hegazy K A, Elswaidy N R, Kassab A A, Elbakary N. The Effect of Energy Drinks and Their Withdrawal on the Renal Cortex of Adult Male Albino Rats. *Histological, Ultrastructural and Morphometric Study*. *Egyptian Journal of Histology*. (2023); 46(3), 1282-95.
 59. Ashari S, Karami M, Shokrzadeh M, Ghandadi M, Ghassemi-Barghi N, Dashti A, Mohammadi H. The implication of mitochondrial dysfunction and mitochondrial oxidative damage in di (2-ethylhexyl) phthalate induced nephrotoxicity in both in vivo and in vitro models. *Toxicology mechanisms and methods*. (2020); 30(6), 427-37.
 60. Abdelrahman S A, Khattab M A, Youssef M S, Mahmoud A A. Granulocyte-colony stimulating factor ameliorates di-ethylhexyl phthalate-induced cardiac muscle injury via stem cells recruitment, Desmin protein regulation, antifibrotic and antiapoptotic mechanisms. *Journal of Molecular Histology*. (2023); 54(4), 349-63.
 61. Saleh S M, Mahmoud A B, Al-Salahy M B, Mohamed Moustafa F A. Morphological, immunohistochemical, and biochemical study on the ameliorative effect of gallic acid against bisphenol A-induced nephrotoxicity in male albino rats. *Scientific Reports*. (2023); 13(1), 1730-8.
 62. Amara I, Scuto M, Zappalà A, Ontario M L, Petralia A, Abid-Essefi S, Calabrese V. *Hericium erinaceus* prevents DEHP-induced mitochondrial dysfunction and apoptosis in PC12 cells. *International journal of molecular sciences*. (2020); 21(6), 2130-9.
 63. Dai X Y, Zhu S Y, Chen J, Li M Z, Talukder M, Li J L. Role of toll-like receptor/MyD88 signaling in lycopene alleviated di-2-ethylhexyl phthalate (DEHP)-induced inflammatory response. *Journal of Agricultural and Food Chemistry*. (2022); 70(32), 10022-30.
 64. Li S, Gu X, Zhang M, Jiang Q, Xu T. Di (2-ethylhexyl) phthalate and polystyrene microplastics co-exposure caused oxidative stress to activate NF-κB/NLRP3 pathway aggravated pyroptosis and inflammation in mouse kidney. *Science of The Total Environment*. (2024); 926, 1-12.
 65. El-haleem A, Manal R, Kattaia A A, El-Baset A, Samia A, El Sayed Mostafa H. Alleviative effect of myricetin on ochratoxin A-induced oxidative stress in rat renal cortex: histological and biochemical study (2016); 31(4), 441–451.
 66. Ali A F, Ghoneim N S, Salama R. Light and electron microscopic study on the effect of Gibberellic acid on the renal cortex of adult male albino rats and the possible protective role of coenzyme Q10. *Egyptian Journal of Histology*. (2021); 44(2), 368-83.
 67. Isaac M R. Effects of Anabolic Steroids on the Histological Structure of Renal Cortex of Adult Male Albino Rats and the Possible Protective Role of Taurine. *Egyptian Journal of Histology*.

- (2019); 42(2), 346-57.
68. Witherel C E, Abebayehu D, Barker T H, Spiller K L. Macrophage and fibroblast interactions in biomaterial-mediated fibrosis. *Advanced healthcare materials*. (2019); 8(4), 1-16.
 69. El-Haroun H, Bashandy M A, Soliman M A E. Impact of remdesivir on the kidney and potential protective capacity of granulocyte-colony stimulating factor versus bone marrow mesenchymal stem cells in adult male albino rats. *Egyptian journal of Histology*. (2022); 45(2), 338-58.
 70. Abd El-Baset S A, Mazen N F, Abdul-Maksoud R S, Kattaia A A. The therapeutic prospect of zinc oxide nanoparticles in experimentally induced diabetic nephropathy. *Tissue barriers*. (2023); 11(1), 1-21.
 71. Shi H, Zhao X, Peng Q, Zhou X, Liu S, Sun C, Sun S. Green tea polyphenols alleviate kidney injury induced by di (2-ethylhexyl) phthalate in mice. *American Journal of Nephrology*. (2024); 55(1), 86-105.
 72. Bekheet E A. Role of Silymarin in ameliorating the harmful effects of Diclofenac sodium on renal cortex of the adult male albino rat: Histological and immunohistochemical study. *The Egyptian Journal of Anatomy*, (2020); 43(1), 106-25.
 73. El-Mahalaway A M. Protective effect of curcumin against experimentally induced aflatoxicosis on the renal cortex of adult male albino rats: a histological and immunohistochemical study. *International journal of clinical and experimental pathology*, (2015); 8(6), 6010-9.
 74. Huang H, You Y, Lin X, Tang C, Gu X, Huang M, Huang F. Inhibition of TRPC6 signal pathway alleviates podocyte injury induced by TGF- β 1. *Cellular Physiology and Biochemistry*, (2017); 41(1), 163-72.
 75. Fadda W A, Essawy A S, Faried M A. Green tea extract protects the renal cortex against bisphenol A-induced nephrotoxicity in the adult male albino rat: a histological and immunohistochemical study. *Eur J Anat*, (2019); 23(6), 415-24.
 76. Terada N, Karim M R, Izawa T, Kuwamura M, Yamate J. Expression of β -catenin in regenerating renal tubules of cisplatin-induced kidney failure in rats. *Clinical and Experimental Nephrology*. (2018); 22, 1240-50.
 77. Saxena S, Dagar N, Shelke V, Puri B, Gaikwad A B. Wnt/beta-catenin modulation: A promising frontier in chronic kidney disease management. *Fundamental & Clinical Pharmacology*, 38(6), (2024); 1020-30.
 78. Üstündağ, Ü V, Emekli-Alturfan E. Wnt pathway: A mechanism worth considering in endocrine disrupting chemical action. *Toxicology and Industrial Health*, (2020); 36(1), 41-53.
 79. Hu X X, Yin Y C, Xu P, Wei M, Zhang W. Network toxicology and cell experiments reveal the mechanism of DEHP-induced diabetic nephropathy via Wnt signaling pathway. *Toxicology and Applied Pharmacology*. (2024); 493, 1-11.
 80. Şener Akçora D, Erdoğan D, Take Kaplanoğlu G, Göktaş G E, Şeker U, Elmas Ç. Electron microscopic investigation of benzo (a) pyrene-induced alterations in the rat kidney tissue and the protective effects of curcumin. *Ultrastructural Pathology*. (2022); 46(6), 519-30.
 81. Bayoumi A, Yassa H, Mohamed R, El-sebaie M, Mousa A, Hassan D. Nanocurcumin: A Promising Therapeutic Supplements Lessening Cadmium-Induced Lung Injury Of Adult Male Albino Rat. A Histopathological, Biochemical and Ultra-structural Study. *Journal of Medical Histology*. (2021); 5(1), 88-92.
 82. Guo S, Meng X W, Yang X S, Liu X F, Ou-Yang C H, Liu C. Curcumin administration suppresses collagen synthesis in the hearts of rats with experimental diabetes. *Acta Pharmacologica Sinica*. (2018); 39(2), 195-204.
 83. Embaby A, Abdel-Kawi S. Histological Study on the Effect of Curcumin and Curcumin Nanoparticles on Cadmium-Induced Liver Damage in Adult male Albino Rats. *Journal of Medical Histology* (2021); 5(2), 119-33.
 84. Atia M M, Abdel-Tawab H S, Mostafa A M, Mobarak S A. The Immunomodulatory Role of Curcumin and Its Nanoparticles in Mice Testis Exposed to N, N'-Methylenebisacrylamide. *Egyptian Academic Journal of Biological Sciences, B. Zoology*. (2022); 14(1), 39-54.
 85. Elmasry K, Bondok A A. Possible synergistic effect of curcumin on captopril/losartan combined therapy in diabetic nephropathy. *Zagazig University Medical Journal*. (2024); 30(1.2), 176-89.
 86. Ambacher K K, Pitzul K B, Karajgikar M, Hamilton A, Ferguson S S, Cregan S P. The JNK-and AKT/GSK3 β -signaling pathways converge to regulate Puma induction and neuronal apoptosis induced by trophic factor deprivation (2012) ;7(10), 1-14.
 87. Tao H, Yang J J, Shi K H, Li J. Wnt signaling pathway in cardiac fibrosis: new insights and directions. *Metabolism*. (2016); 65(2), 30-40.
 88. Vallée A, Lecarpentier Y, Vallée J N. Curcumin: a therapeutic strategy in cancers by inhibiting the canonical WNT/ β -catenin pathway. *Journal of Experimental & Clinical Cancer Research*. (2019); 38, 1-16.

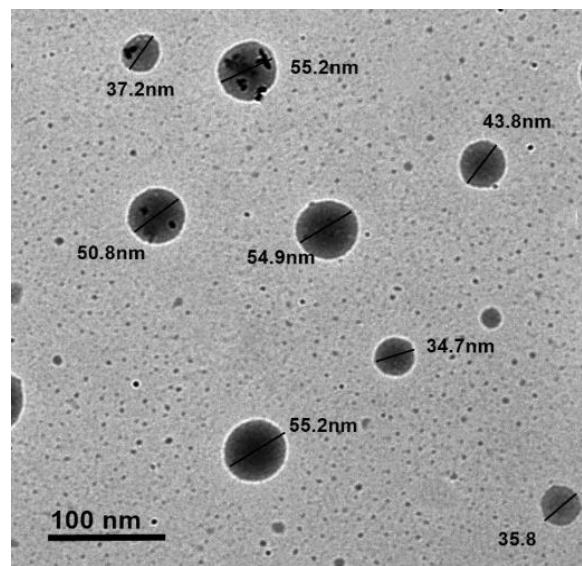


Figure (1s): An electron micrograph showing average diameters (<100 nm) of Nanocurcumin used in the current study.

Citation

Ibrahem, N., Al Hosiny, A., Mohamed, O., Shaheen, M. The Effect of Nanocurcumin on Di-Ethylhexyl Phthalate-Induced Injury in Rats' Renal Cortex (A Histological and Biochemical Study). *Zagazig University Medical Journal*, 2025; (2046-2069): -. doi: 10.21608/zumj.2025.352818.3852